

# Manipulating Crystal Orientation of Poly(ethylene oxide) by Nanopores

Yu Guan,<sup>†</sup> Guoming Liu,<sup>†</sup> Peiyuan Gao,<sup>‡</sup> Li Li,<sup>§</sup> Guqiao Ding,<sup>||</sup> and Dujin Wang<sup>†,\*</sup>

<sup>†</sup>Beijing National Laboratory for Molecular Sciences, CAS Key Laboratory of Engineering Plastics, Institute of Chemistry, Chinese Academy of Sciences, Beijing, 100190, China

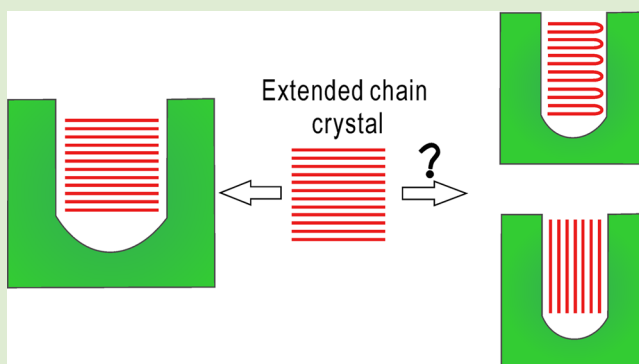
<sup>‡</sup>Beijing National Laboratory for Molecular Sciences, State Key Laboratory of Polymer Physics and Chemistry, Institute of Chemistry, Chinese Academy of Sciences, Beijing, 100190, China

<sup>§</sup>Shanghai Synchrotron Radiation Facility, Shanghai Institute of Applied Physics, Chinese Academy of Sciences, Shanghai, 201204, China

<sup>||</sup>State Key Laboratory of Functional Materials for Informatics, Shanghai Institute of Microsystem and Information Technology, Chinese Academy of Sciences, Shanghai, 200050, China

## Supporting Information

**ABSTRACT:** The confined crystallization behavior of a low molecular weight monodisperse polyethylene oxide (PEO) in anodic alumina oxide (AAO) templates was investigated. Homogeneous nucleation of polymer in AAO templates was confirmed. Within AAO with diameter larger than the contour length of PEO chains, the “kinetics selective growth” crystallization mechanism was confirmed based on the observation that the chain axis preferentially aligned perpendicular to the pore axis. However, when AAO diameter further decreases to a value smaller than the contour length of PEO, unique orientation with chain axis aligned parallel to the pore axis was observed for the first time. The results were discussed based on the competition between thermodynamics and kinetics during the crystallization process.



Nanostructured materials have become a hot research focus in material science because of various attractive properties and their enormous potential applications.<sup>1–5</sup> For crystalline polymers, the crystalline phase is usually decisive for many properties. It has been found that polymer under nanoconfinement exhibits unique crystallization behavior, including variation of nucleation mechanism,<sup>6–11</sup> orientation,<sup>7,9,11,12</sup> and decreased crystallinity.<sup>9,10,12</sup> Among various confining circumstances, anodic alumina oxide (AAO) templates,<sup>13</sup> with nanoscale cylinder arrays, have been widely used for producing 1D nanorods/nanotubes. AAO templates can be prepared in large scale and can be easily infiltrated with various polymer melts.<sup>14–16</sup> Additionally, the uniform cylinders in AAO are size-controllable with good mechanical strength and high thermostability. All the above features make AAO an ideal system for studying the crystallization behavior of polymers under confinement.

The crystallinity of polymers confined in AAO is generally lower than that in the bulk state.<sup>9,10,12</sup> With decreasing pore diameter, the crystallinity continuously goes down. Besides, a drastic decrease of crystallization temperature for polymers confined in AAO is frequently observed, which was generally regarded as a sign for a transition from heterogeneous to homogeneous nucleation.<sup>10,11</sup> Another important observation is

that the crystallization of the polymer in AAO is anisotropic. The polymer chains (normally, *c*-axis) align preferentially perpendicular to the AAO pore axis.<sup>7,9,11</sup> In other words, the lamellae grow along with the AAO pore axis. Steinhart et al.<sup>7</sup> have proposed a theoretical scenario to explain the oriented crystallization. Within the AAO pores, homogeneous nucleation produces nuclei randomly. Then only the crystals with the  $\langle hk0 \rangle$  direction aligned with the long axis of pores are able to grow. Lamellae with an  $\langle hkl \rangle$  direction where *l* is nonzero are “blocked” by the rigid wall. Additionally, some reports<sup>11,17</sup> stressed the influence of possible surface-induced nucleation on the crystallization of polymers in AAO.

The reported results repeatedly verify that polymer lamellae adopt a specific orientation with the *c*-axis preferentially aligned perpendicular to the long axis of the AAO pores. Similar to some other facts in polymer physics such as folded chain crystal, polymorphism, and multiphase morphology, this could be seen as another paradigm of kinetics-controlled phenomenon. However, a fundamental question is what would happen if

Received: November 8, 2012

Accepted: February 8, 2013

Published: February 14, 2013

kinetics-favored conformations are not thermodynamically stable in confined crystallization. Figure 1 shows the possible

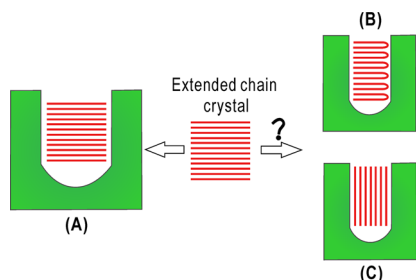


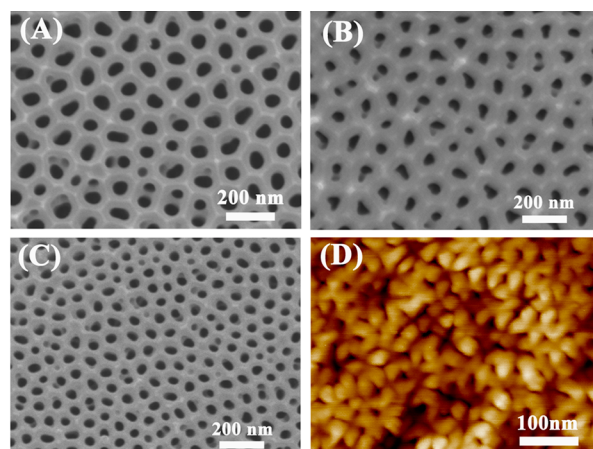
**Figure 1.** Schematic illustration of the possible packing modes of a monodisperse low molecular weight polymer in different AAO templates. (A) In an AAO template with pore diameter larger than the contour length of the polymer chain, it is most likely that the chain axis would align perpendicular to the pore axis. In an AAO template with pore diameter smaller than the contour length of the polymer chain, two packing modes are possible: (B) the chain axis aligns perpendicular to the pore axis and the chains are folded (both integer and noninteger folding are possible), (C) or else, the chain axis aligns parallel to the pore axis with an extended conformation.

packing modes of a monodisperse low molecular weight polymer in different AAO templates. The low molecular weight polymer exhibits extended chain crystal in bulk. If the AAO pore diameter is larger than the contour length of the polymer chain, it is reasonable to hypothesize that lamellae would probably adopt an orientation with chains preferentially aligned perpendicular to the pore axis. That means the  $\langle 120 \rangle$  direction, the fastest growth direction of PEO crystals, grows parallel to the pore axis and dominates the overall orientation (Figure 1A). However, the situation becomes complicated if the AAO pore size decreases to a value smaller than the chain's contour length. To maintain the kinetically controlled orientation, the chains have to fold back because of the spatial confinement (Figure 1B). Those chain conformations are obviously thermodynamically unfavorable. On the other hand, if the chains form a thermodynamically stable extended crystal as depicted in Figure 1C, the growth of the crystal is kinetically difficult since the  $\langle 120 \rangle$  direction of PEO crystals grows perpendicularly to the pore axis.

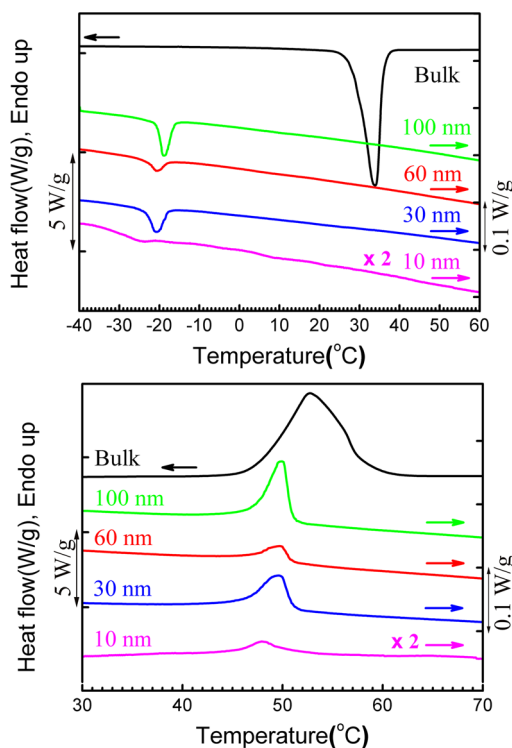
To clarify the packing mode of polymer crystals in different sized confined spaces, we constituted a model system with low molecular weight poly(ethylene oxide) (PEO) with extended chain length of 12.6 nm and AAO templates with different pore diameters (the lowest one is 10 nm). For the first time, the crystal orientation with the  $c$ -axis aligned parallel to the long axis of AAO pores was observed in the AAO ( $\Phi = 10$  nm). The current observation may give new insight into the understanding of the crystallization behavior of crystalline polymers under nanoscale confinement.

Figure 2 shows the SEM and AFM images of the surface of four AAO templates. The pore size is relatively uniform. The average diameters of the AAO templates are  $\Phi = 100$ , 60, 30, and 10 nm, as shown in Figure 2(A)–(D), respectively. For the AAO template with  $\Phi = 10$  nm, the pore depth is  $\sim 20$   $\mu\text{m}$ , while for all other templates, the pore depth is larger than 65  $\mu\text{m}$ .

Figure 3 shows the differential scanning calorimetry (DSC) cooling and heating curves of PEO in the AAO templates. Bulk PEO exhibits a strong and sharp exothermic crystallization peak at  $\sim 34$   $^{\circ}\text{C}$ . For the PEO in the AAO templates with pore



**Figure 2.** SEM and AFM images of AAO templates with different pore diameters: (A) 100 nm, (B) 60 nm, (C) 30 nm, and (D) 10 nm.



**Figure 3.** DSC cooling (A) and heating (B) thermograms of bulk PEO and PEO confined in AAO templates. For clarity, the heat flow of PEO confined in AAO with diameter of 10 nm was multiplied by a factor of 2. The DSC curves were normalized by the weight of both the PEO and AAO template.

diameter of 100, 60, and 30 nm, the crystallization peak temperature shifts substantially to around  $-20$   $^{\circ}\text{C}$ . The peak temperatures of PEO in various AAO templates are listed in Table 1. The drastic decrease of crystallization temperature is a

**Table 1.** Crystallization and Melting Temperatures of Bulk PEO and PEO Confined in AAO Templates with Different Pore Diameters

| samples                      | bulk PEO | 100 nm | 60 nm | 30 nm | 10 nm |
|------------------------------|----------|--------|-------|-------|-------|
| $T_c$ ( $^{\circ}\text{C}$ ) | 34.0     | -18.6  | -20.7 | -21.0 | -25.1 |
| $T_m$ ( $^{\circ}\text{C}$ ) | 52.7     | 49.8   | 49.7  | 49.6  | 47.9  |

typical feature for polymers in confined spaces. One straightforward explanation is the transition of the nucleation mechanism, e.g., from heterogeneous to homogeneous. The nucleating heterogeneities in the bulk sample can easily initiate crystallization, and the crystallization spreads out until boundary impingement. For polymer confined in AAO, the melt is divided by templates into numerous nanoscale domains, in which each heterogeneous site can only influence an “infinitesimal” fraction of matter. Statistically, homogeneous nucleation dominates the overall crystallization process, which needs a larger supercooling to overcome the larger free energy barrier.<sup>6,10,18</sup> As shown in Table 1, the crystallization temperature decreases with decreasing pore diameter. This is in accordance with the relationship in the criteria of homogeneous nucleation<sup>19</sup> (detailed discussions can be found in the Supporting Information). The melting temperatures of the PEO in AAO are similar to each other, all of which are  $\sim 4$  °C lower than that of bulk.

To reveal the orientation of the PEO crystals within the AAO nanopores, 2D WAXD experiments were carried out at room temperature (Figure 4). Figure 4(A) is a schematic illustration

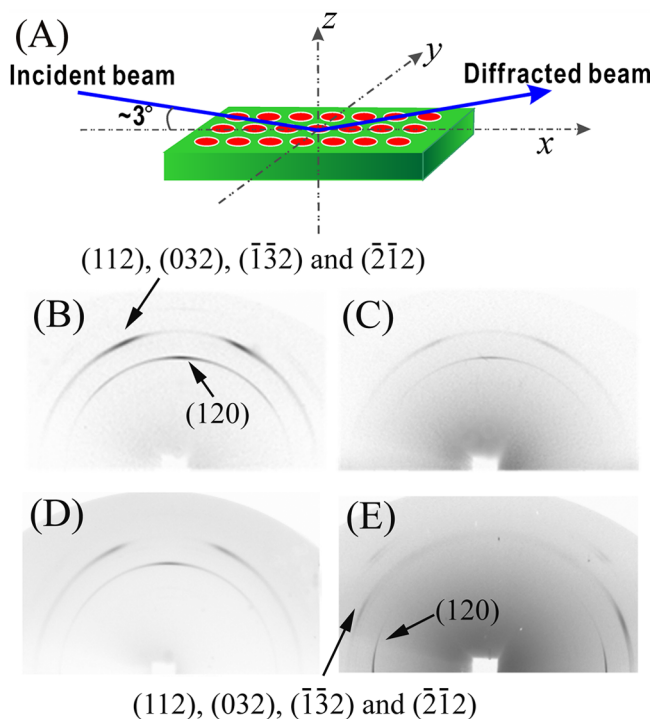


**Figure 4.** Schematic illustration of the experimental geometry of the WAXD measurements (A). X-ray incident angle with respect to the template is 3°. 2D WAXD patterns of PEO confined within the different sized AAO templates: (B) 100 nm, (C) 60 nm, (D) 30 nm, and (E) 10 nm.

of the experimental setup of the measurement. The normal of the plane for the AAO surface is defined as the  $z$  axis, while two lines in the AAO surface perpendicular to each other are defined as the  $x$  and  $y$  axes. The selection of the  $x$  and  $y$  axes is random based on the symmetry.

Figure 4(B–E) shows the 2D WAXD patterns of the PEO infiltrated in the AAO templates. As seen in Figure 4(B), two strong reflections were observed. The reflections have  $d$  spacing values of 4.59 and 3.78 Å, which can be assigned to the 120 and 112/032/1̄1̄3̄2/2̄1̄1̄2 reflections, respectively. The reflection

patterns of the PEO in the 30, 60, and 100 nm AAO pores are similar. The 120 reflection locates at the meridian, and the 112/032/1̄1̄3̄2/2̄1̄1̄2 reflections locate on the off-meridian positions. These patterns are in well accordance with the previous reports.<sup>10,20</sup> The  $c$ -axis of the PEO chains preferentially aligns perpendicular to the pore axis. In other words, the lamellae grow along the AAO nanopores. However, it is striking to find that the PEO in the 10 nm AAO displays a completely different diffraction pattern. The 120 reflection locates at the equator, and the 112/032/1̄1̄3̄2/2̄1̄1̄2 reflections move accordingly. These patterns correspond to an orientation with the  $c$  axis preferentially aligning parallel to the pore axis.

The packing mode of the PEO lamellae with  $c$ -axis perpendicular to the AAO pore axis can be readily explained by the “kinetics selective growth” theory.<sup>7</sup> Upon cooling, PEO nucleates randomly. Because of the 1D geometry, lamellae with the  $\langle hk0 \rangle$  direction in parallel to the AAO pore axis can grow gradually. Crystallites with other orientations would stop growing when the growth front encounters the wall of the AAO. This mechanism has an obvious prerequisite: the thickness of the lamellae should be smaller than the diameter of the AAO pores. The extended chain length of the PEO in the present study is 12.6 nm. Under the condition of the AAO with diameter larger than 12.6 nm (Figure 1A), it could be expected that AAO does not provide thermodynamic constraints on the crystallization of the PEO. Therefore, the “kinetics selective growth” mechanism determines the orientation of lamellae. On the contrary, for the AAO with a 10 nm diameter, the chain contour length is greater than the pore diameter, so the constraint applied on PEO is intrinsically different. The PEO chains have to face a dilemma. The growth of lamellae with the  $\langle hk0 \rangle$  direction in parallel to the pore axis is kinetically favored. To achieve such an orientation, a folded chain conformation is required. However, it is known that lamellae with a folded chain in the investigated PEO are thermodynamically unstable in the bulk state compared to the extended chain lamellae. Ultimately, the final structure results from the competition between the kinetics and thermodynamics processes. Our results show that the PEO lamellae adopt a structure with the thermodynamic preference, with the PEO chains aligning in parallel to the pore axis of AAO to preserve the extended chain conformation (Figure 1C).

It should be pointed out that the stability of polymer lamellae is generally believed to depend on the thickness, according to the well-known Gibbs–Thomson equation<sup>21,22</sup>

$$T_m = T_m^0 \left( 1 - \frac{2\sigma_e}{l\Delta H} \right)$$

where  $T_m$  is the melting point;  $T_m^0$  is the equilibrium melting point;  $\sigma_e$  is the folded surface free energy;  $l$  is the lamellar thickness; and  $\Delta H$  is the enthalpy of fusion. At a first glance, one might assume that the PEO in AAO has thinner lamellae via chain folding. However, in the Gibbs–Thomson equation, the lateral surface free energy is omitted for simplicity (Figure S2, Supporting Information), which is generally valid in bulk polymers. In our case, PEO lamellae confined in nanoscale channels would be highly fragmented. The large lateral surface area, with higher free energy than that of bulk, is attributed to the relatively low  $T_m$  of PEO in AAO.

To further understand the unique orientation behavior, we calculated the energies of the extend chain crystal and the once folded chain crystal of the PEO with a molecular mechanics simulation using the COMPASS force field. A microcrystal

consisting of 12 PEO chains with 45 monomers ( $M_w = 1998$  g/mol) was considered as the model system (Figure S3, Supporting Information). To simplify the calculation, the interaction between the PEO chains and the aluminum oxide wall were not taken into account. The unit cell parameters of the extended chain crystal and the folded chain crystal were supposed to be the same, hence both of which were set to be the same as the bulk monoclinic modification.<sup>20</sup> It was assumed that the chain folding is adjacent to reentry within the 120 plane, according to the previous reports.<sup>23,24</sup> The conformations of the monomers at the folded surface were optimized to obtain a relatively stable state.

Table 2 shows the calculated results. It can be seen that both the chain conformation energy and the intermolecular energy

**Table 2. Total Energy of PEO Chain Confined in the AAO Templates: Extended Chain vs Folded Chain**

|                                | extended chain | once folded chain |
|--------------------------------|----------------|-------------------|
| conformational energy/(kJ/mol) | -213           | 3844              |
| intermolecular energy/(kJ/mol) | -2719          | 6903              |
| total energy/(kJ/mol)          | -2932          | 10747             |

for the once folded chain crystal are much higher than those for the extend chain crystal. This indicates that the crystal with folded chains of PEO with  $M_w = 2000$  g/mol is unstable compared to the extend chain crystal. In fact, the folded chain crystal for the PEO with  $M_n$  smaller than 2000 g/mol has never been observed experimentally before. Our investigation shows that, under the competition between thermodynamics and kinetics processes, the PEO crystallizing in an AAO with a diameter smaller than the chain contour length adapts a thermodynamically stable conformation with the chain axis aligning in parallel to the pore axis.

In conclusion, this study examined the crystallization of a low molecular weight monodisperse polyethylene oxide (PEO) in the anodic alumina oxide (AAO) templates with a range of pore diameters from 100 nm down to 10 nm, which is the smallest pore diameter among the AAO templates ever reported in confined crystallization research. Within the 10 nm AAO, a unique chain orientation of the PEO has been identified for the first time; i.e., the chain axis aligns in parallel to the pore axis. Within an AAO with pore diameter larger than the contour length of the PEO chains, lamellae are packed with the chain axis preferentially aligning perpendicular to the AAO pore axis, which is in line with the “kinetics selective growth” theory. Furthermore, the change of the chain orientation mode within an AAO with a pore diameter smaller than the contour length of the PEO chains confirms the crystallization transformation from kinetics control to thermodynamics priority. The understanding of the polymer crystallization behavior under nanoconfinement will provide theoretical guidance for manipulating nanostructures and nanomaterials with functional properties.

## ■ ASSOCIATED CONTENT

### Supporting Information

Materials, sample preparation, characterization, detail analysis of crystallization/melting behavior and molecular simulation models are indicated in the text. This material is available free of charge via the Internet at <http://pubs.acs.org>.

## ■ AUTHOR INFORMATION

### Corresponding Author

\*E-mail: [djwang@iccas.ac.cn](mailto:djwang@iccas.ac.cn).

### Notes

The authors declare no competing financial interest.

## ■ ACKNOWLEDGMENTS

Financial support from the National Natural Science Foundation of China (50925313, 21274156, and 51203170) and ICCAS (CMS-PY-201218) is gratefully acknowledged. The SSRF is acknowledged for kindly providing the beam time.

## ■ REFERENCES

- (1) Ibn-Elhaj, M.; Schadt, M. *Nature* **2001**, *410*, 796–799.
- (2) Choi, J.; Luo, Y.; Wehrspohn, R. B.; Hillebrand, R.; Schilling, J.; Gosele, U. *J. Appl. Phys.* **2003**, *94*, 4757–4762.
- (3) Mayes, A. M. *Nat. Mater.* **2005**, *4*, 651–652.
- (4) Rittigstein, P.; Priestley, R. D.; Broadbelt, L. J.; Torkelson, J. M. *Nat. Mater.* **2007**, *6*, 278–282.
- (5) Wang, H. P.; Keum, J. K.; Hiltner, A.; Baer, E.; Freeman, B.; Rozanski, A.; Galeski, A. *Science* **2009**, *323*, 757–760.
- (6) Loo, Y. L.; Register, R. A.; Ryan, A. J.; Dee, G. T. *Macromolecules* **2001**, *34*, 8968–8977.
- (7) Steinhart, M.; Goring, P.; Dernaika, H.; Prabhakaran, M.; Gosele, U.; Hempel, E. *Phys. Rev. Lett.* **2006**, *97*, No. 027801.
- (8) Woo, E.; Huh, J.; Jeong, Y. G.; Shin, K. *Phys. Rev. Lett.* **2007**, *98*, No. 136103.
- (9) Shin, K.; Woo, E.; Jeong, Y. G.; Kim, C.; Huh, J.; Kim, K. W. *Macromolecules* **2007**, *40*, 6617–6623.
- (10) Duran, H.; Steinhart, M.; Butt, H. J.; Floudas, G. *Nano Lett.* **2011**, *11*, 1671–1675.
- (11) Michell, R. M.; Lorenzo, A. T.; Muller, A. J.; Lin, M. C.; Chen, H. L.; Blaszczyk-Lezak, L.; Martin, J.; Mijangos, C. *Macromolecules* **2012**, *45*, 1517–1528.
- (12) Wu, H.; Wang, W.; Yang, H. X.; Su, Z. H. *Macromolecules* **2007**, *40*, 4244–4249.
- (13) Masuda, H.; Fukuda, K. *Science* **1995**, *268*, 1466–1468.
- (14) Martin, C. R. *Science* **1994**, *266*, 1961–1966.
- (15) Steinhart, M.; Wendorff, J. H.; Greiner, A.; Wehrspohn, R. B.; Nielsch, K.; Schilling, J.; Choi, J.; Gosele, U. *Science* **2002**, *296*, 1997–1997.
- (16) Steinhart, M. *Adv. Polym. Sci.* **2008**, *220*, 123–187.
- (17) Wu, H.; Wang, W.; Huang, Y.; Su, Z. H. *Macromol. Rapid Commun.* **2009**, *30*, 194–198.
- (18) Wunderlich, B. *Macromolecular Physics. Crystal Nucleation, Growth, Annealing*; Academic: New York, 1976; Vol. 2.
- (19) Müller, A. J.; Balsamo, V.; Arnal, M. L. *Adv. Polym. Sci.* **2005**, *190*, 1–63.
- (20) Takahashi, Y.; Tadokoro, H. *Macromolecules* **1973**, *6*, 672–675.
- (21) Stranski, I. N.; Kaischew, R. *Z. Phys. Chem. B* **1934**, *26*, 100–113.
- (22) Kaischew, R.; Stranski, I. N. *Z. Phys. Chem. B* **1937**, *35*, 427–432.
- (23) Kovacs, A. J.; Straupe, C.; Gonthier, A. *J. Polym. Sci., Polym. Symp.* **1977**, *59*, 31–54.
- (24) Chen, J. H.; Cheng, S. Z. D.; Wu, S. S.; Lotz, B.; Wittmann, J. C. *J. Polym. Sci., Part B: Polym. Phys.* **1995**, *33*, 1851–1855.